Methods to mitigate railway premium fastening system spike fatigue failures using finite element analysis

Marcus S. Dersch [*], Christian Khachaturian, J. Riley Edwards

Rail Transportation and Engineering Center – RailTEC, Department of Civil and Environmental Engineering – CEE, Grainger College of Engineering – GcoE, University of Illinois at Urbana-Champaign – UIUC, 1240 Newmark Civil Engineering Laboratory, MC-250, 205 N. Mathews Ave., Urbana, IL 61801, USA

ABSTRACT

Railroad track fasteners work as a system, in conjunction with the sleeper, to maintain gauge, transmit loads, and resist lateral and longitudinal rail movement. Timber sleeper elastic fastening systems have shown benefits by preventing rail rollover derailments and reducing spike killing. However, these systems have experienced broken spike failures leading to at least 10 derailments over the past 20 years. Recent studies focusing on the cause of the failures have indicated that the spikes fail in fatigue and these fatigue failures are driven by the addition of longitudinal loads the spikes carry. Further, due to the nature of the elastic fastener, the wave-action of the rail separates the plate from the sleeper, as opposed to the rail from the plate, thus eliminating the load transferred by friction. This study quantifies the effect of fastening system design changes on spike stress and the load required to exceed the spike endurance limit. Specific design changes investigated in this study include increasing spike cross-sectional area, comparing spike type (cut vs screw), varying the spike load location, controlling the development of friction between the sleeper and plate, varying spike engagement and finally, adjusting the quantity of spikes at a given rail seat. Finite element analysis (FEA) was used to quantify these effects and multiple 3D models were developed and used. Results indicate that the two most effective methods to reduce spike stress and increase the required load to exceed the spike's endurance limit, and thus mitigate spike fatigue failures, would be to ensure spike engagement between the plate and spikes and develop friction between the plate and sleeper (e.g. add spring washers, etc.). Future fastening system designs can incorporate these, and other findings, to mitigate spike fastener failures to ensure the full value of timber sleeper elastic track fastening systems is realized.

1. Introduction

Ballasted track is commonly used throughout the world and consists of the rail, fastening systems, crossties, ballast, sub-ballast, and subgrade [1]. Rail fastening systems, in conjunction with the sleeper, secure the rail to maintain gauge, transmit the thermal and service loads, and anchor the rail-sleeper structure against lateral and longitudinal movements [1,2]. Timber sleeper fastening systems consisting of an elastic fastener (e.g. e-clip, tension clamp, etc.) and spikes (e.g. cut, screw, drive, etc.) have shown benefits in preventing rail rollover derailments and reductions in spike kill [2,3].

---

* Corresponding author.
E-mail addresses: mdersch2@illinois.edu (M.S. Dersch), Ckhacha2@illinois.edu (C. Khachaturian), jedward2@illinois.edu (J.R. Edwards).

However, timber sleeper elastic fastening systems have experienced broken spike failures that have led to at least 10 derailments over the past 20 years in North America [4]. With the installation of these systems increasing over the past few years, there has been an increased focus on quantifying the mechanics of spike failures and methods to mitigate them to increase the safety of the track system. Recent spike failure studies [3–6] have indicated that these elastic fastening systems must transfer lateral and longitudinal loads, as opposed to mainly lateral loads only. The addition of the longitudinal loads lead to spike stresses exceeding the endurance limit and failing in fatigue. Further, due to the design of the elastic fastener within the elastic system, the wave action of the rail leads to a separation of the plate from the sleeper eliminating transfer of forces by friction [7]; thus ensuring the longitudinal load is transferred directly to the spikes.

Given that the failures have been classified as fatigue failures, reducing the stress state of the spike below the endurance limit is critical for mitigation. Therefore, this paper provides data that could be implemented in future fastening system designs to mitigate the fatigue failures through spike stress reductions. This is accomplished through investigating methods to reduce the spike stress state using 3D finite element analysis (FEA) leveraging a validated model presented by Dersch et al. [4]. Methods to mitigate spike stresses considered within this paper include:

- Spike cross-sectional area
- Spike type (cut vs screw)
- Spike loading location
- Plate normal (vertical) clamping force
- Spike engagement with plate & quantity of spikes within a given fastening system

2. Purpose

The methods investigated in this paper are not considered to be exhaustive. For example, recent studies have also investigated the effect of timber material and loading direction [4,8], and thus were not the focus of this study. However, the following sections provides engineering reason and justification for the investigations considered.

2.1. Spike cross-sectional area

Given that this is a flexural fatigue problem it is important to remember that the maximum bending stress for Euler-Bernoulli beams is related to both the demand on the component and its geometry (Equation (1)). Reductions in stress would result from decreasing the bending moment, increasing the distance from the outermost surface of the spike to the neutral axis, and/or increasing the moment of inertia of the spike.
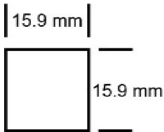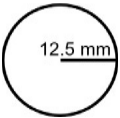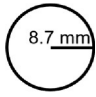
$$\sigma = \frac{My}{I} \tag{1}$$

where

σ = maximum normal stress
M = bending moment
y = distance from the neutral axis
I = area moment of inertia

Increasing the cross-sectional area of the spike would reduce the maximum stress within the spike given it increases the ratio of the distance from the neutral axis to the area moment of inertia. Though this is an obvious solution based on mechanics, the FEA results below quantify the effectiveness of this solution. Further, there are limits to the feasible increase in spike cross-sectional area before splitting the timber becomes a concern.

Table 1
Comparison of geometric characteristics and resulting demands on standard cut and screw spikes.

Spike (type/location)	Cut	Screw (Upper Shaft)	Screw (Threads)
Cross Section	15.9 mm × 15.9 mm	12.5 mm	8.7 mm
Area Moment of Inertia Formula	$bh^3/12$	$\pi r^4/4$	$\pi r^4/4$
I (mm^4)	5,293	19,077	4,565
y (mm.)	7.9	12.5	8.7
Stress (force/mm^2)	$0.0015 \times M^*$	$0.0007 \times M^*$	$0.0019 \times M^*$

* where M represents the internal moment in force-in.

2.2. Spike type (cut vs screw)

Even though failures of both systems have been found in the field multiple railroads are transitioning from traditional cut spikes to screw spikes and at least one railroad has recently moved from screw spikes to cut spikes [7]. The geometry and resulting stress as a function of moment (M) are presented in Table 1. The moment of inertia is largest for the screw spike upper shaft and smallest at the screw spike threads. Calculated stresses, given an equivalent internal moment, indicate the threaded portion of the screw spike would experience the greatest stress magnitude, more than 25% greater than the standard cut spike. This appears to align with field measurements indicating that cut spikes fail 38.1 mm (1.5 in.) below the top of crosstie on average while the screw spikes fail near the first two threads of the threaded region, approximately 50.8 mm (2 in.) below the top of crosstie [4,5].

2.3. Plate normal (Vertical) clamping force

Roadcap et al. [7] hypothesized that plate friction, or lack thereof, plays a critical role in maximum spike stress. As friction is lost due to rail and plate uplift, all longitudinal force would transfer to the spike. Further, the AREA Tie Committee (the predecessor organization to AREMA) recommended that there should be no movement between the sleeper and plate and there should be a firm connection between the sleeper and plate [9]. While cut spikes are not designed to provide any plate clamping force, screw spikes (upon proper installation), are known to provide clamping force to the plate to encourage contact between the plate and the sleeper [5,9]. This design encourages longitudinal loads to transfer through friction at the plate-sleeper interface in addition to spike bending.

Equation (2) provides the basic equation for force transfer through friction. To increase the force taken by friction, one must increase the coefficient of friction or the normal force. The coefficient of friction between the plate and sleeper is nominally 0.7 [10,11].

$$f = \mu N \tag{2}$$

where

f = Friction force
μ = Coefficient of friction
N = Normal force

To address screw spikes loosening over time, while also maintaining the normal force between the plate and sleeper, spring washers have historically been used [9]. A spring washer was loaded in the laboratory and deflection recorded (Fig. 1). The hysteresis can be explained through the permanent deformation of the spring. Even when plate cutting or loosening of the screw occurs, a residual normal force is present to ensure the plate is engaged with the sleeper.

Therefore, to quantify the effect of normal clamping force applied by spring washers, and confirm the importance of the aforementioned hypothesis, two magnitudes of normal forces were applied to the plate while holding the longitudinal load constant.
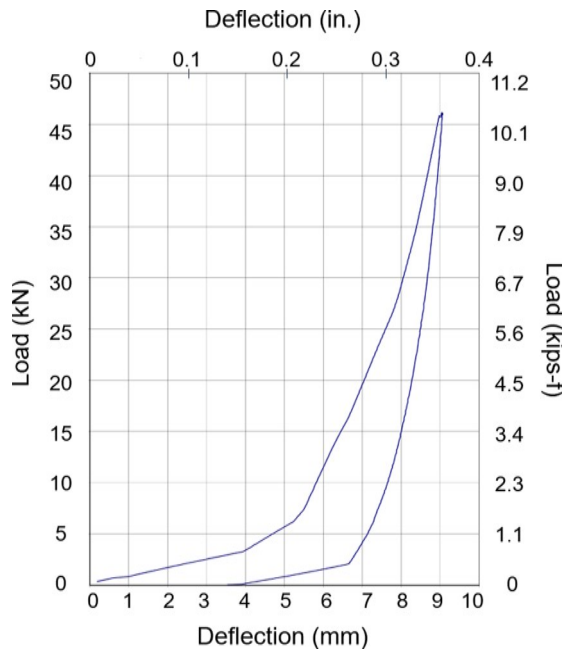

Fig. 1. Example of railroad fastening system spring washer load vs deflection characteristics.

2.4. Spike loading location

The point of spike loading (i.e. plate to spike contact location) is expected to affect spike stress given it would change the length of the moment arm and resulting bending moment. Multiple mechanisms would lead to changes in load contact location; (a) the angle of the spike as driven into the crosstie, (b) the non-planar finished surface of the spike or plate, and (c) plate uplift and/or rotation (Fig. 2). Therefore, to quantify the effect of plate uplift, while maintaining the depth at which the spike was driven, the location of the applied load centroid will be varied while holding the spike installation depth constant.

2.5. Spike engagement with plate and quantity of spikes within a given fastening system

When plate uplift occur, load transfer is only possible when the spike(s) are engaged with the plate (i.e. no friction). The hold-down and line spike holes are 1.65 and 3.18 mm (0.065 in. and 0.125 in.) larger, respectively, than the 15.88 mm (0.625 in.) standard cut spike (Fig. 3). Given the over-sized holes, in combination with findings by Dersch et al. [4] demonstrating the displacement of the spike is not expected to exceed 1.02 mm at 8.90 kN (0.04 in. at 2000 lb.), it is feasible that not all spikes will be in contact with the plate simultaneously.

The lack of engagement of some spikes would lead to a non-uniform force and stress distribution among the spikes. Non-uniform distributions have been reported by Bowman [12] and Gao [13] and the data from their instrumented spike studies indicate a single spike might take between 50 and 70% of the applied force for a single rail seat.

Another factor that could impact the maximum stress within individual spikes is the quantity of spikes used in the fastening system. Currently, standard practice for spiking patterns uses only a subset of available plate holes. For instance, in demanding locations such as curves, special track work, steep grades, etc., four spikes are driven during construction and additional spikes are installed when required for additional strength. As the number of spikes installed per rail seat are increased, the stress in all spikes is expected to be reduced given the total bending strength is increased.

Therefore, to quantify the effect of disengaged spikes within a rail seat system, a parametric study was performed in which spikes were moved from one side of the plate hole to the other and the maximum stress within each spike was quantified. Further, to quantify the effect of increasing the quantity of spikes installed in a given fastening system, a spike was installed in the fifth spike hole in the standard plate shown in Fig. 3, a deviation from current practices.

3. Methodology

FEM has previously been used to successfully quantify the effect of lateral and longitudinal loads on railroad spike stress magnitude and location, and thus was adopted in this study [4]. Abaqus/CAE, a commercially available FEM software package, was selected to perform these simulations.

3.1. Model overview

Three unique models were developed and used for the investigations presented in this paper; Fig. 4 shows a visual representation of each assembled model.

1. Single cut spike-timber block model
2. Single screw spike-timber block model
3. Single rail seat model consisting of multiple spikes, plate, and timber block

The single cut spike-timber block model (Fig. 4, (a)) previously developed and validated by Dersch et al. [4] was used to quantify the effect of spike cross-sectional area, the effect of spike loading location, and effect of spike type. Loading was applied to the spike
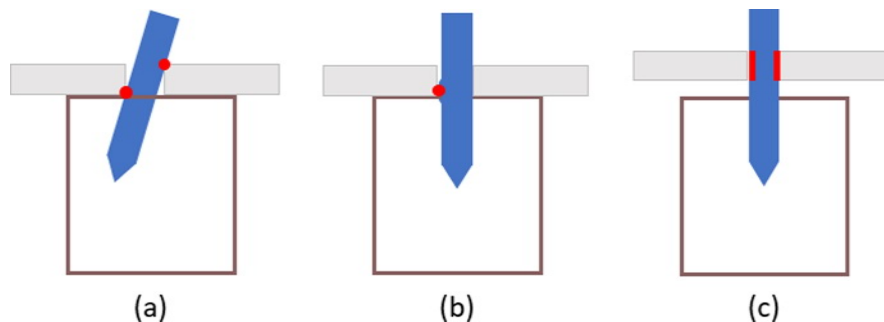

Fig. 2. Potential mechanisms leading to changes in load contact location: (a) a spike driven into the crosstie at an angle, (b) a spike with non-planar finished surface leading to point contact (c) plate uplift and/or rotation which affects load contact location.
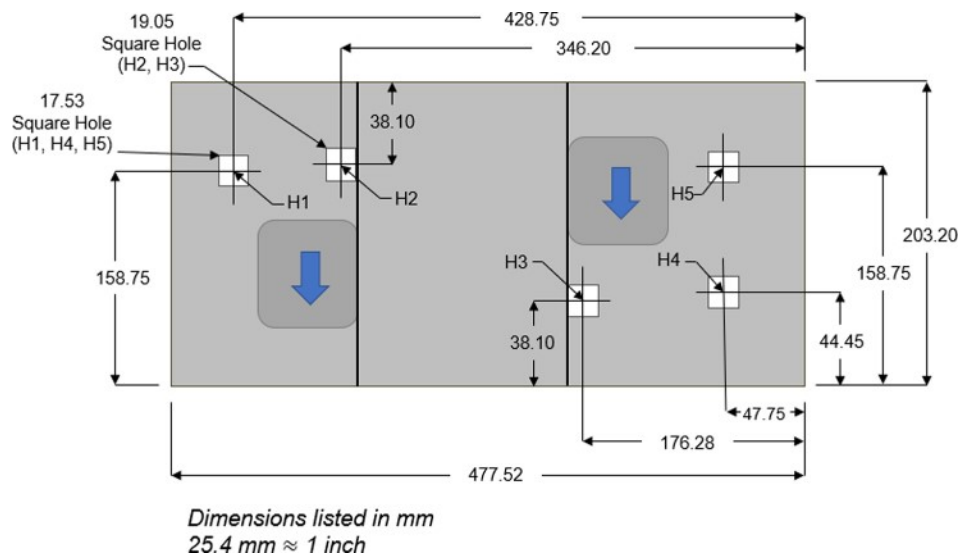
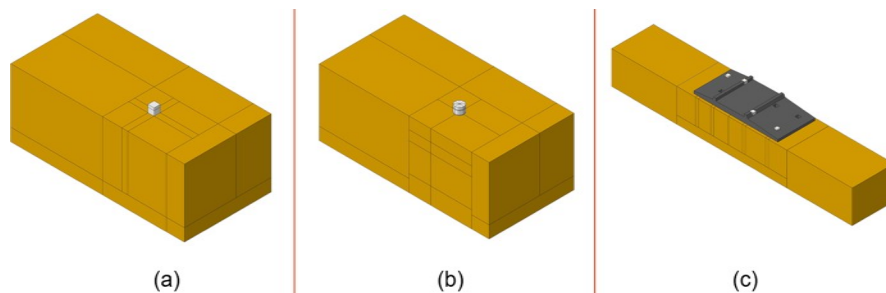**Fig. 3.** Example elastic fastening system plate with dimensions.

Fig. 4. Visual representations of the various assembled FEMs used in this investigation: (a) single cut spike, (b) single screw spike, (c) single rail seat with four spikes.

over a 202 mm^2 (0.3125 in.^{2}) area (15.9 mm × 12.7 mm, (0.625 in. × 0.5 in.)) representing the contact from a sleeper plate. The single screw spike-timber block model (Fig. 4, (b)) incorporated many of the validated portions of the single cut spike-timber block model (timber and spike material properties, mesh densities, boundary conditions, etc.) and was used to quantify the effect of spike type. Loading was applied to a quarter of the screw-spike circumference over a 0.368 in.^{2} area (0.737 in. wide by 0.5 in. tall) representing the contact from a sleeper plate over one-quarter of the circumference of the screw spike. The single rail seat model (Fig. 4, (c)) expanded upon the validated single cut-spike model by increasing the quantity of spikes and adding the plate and was used to quantify the effect of spike engagement with the plate, plate engagement with the sleeper, and number of spikes used within the system. Loading was applied to the plate at the location of the shoulders (see blue arrows within Fig. 3).

3.2. Model details

All components were modeled as 3D deformable solids. The standard cut spikes and timber sleeper were modeled using the validated material properties, mesh densities, boundary conditions presented by Dersch et al. [4]. The standard cut spikes were 152 mm (6 in.) long by 15.9 mm (0.625 in.) square as described within Chapter 5 of the AREMA Manual on Railway Engineering [14]. The standard AREMA recommended Square Head Screw Spike was simplified in the model by removing the threads and head.

Dersch et al. [4] reported the steel Young's Modulus of 212,700 MPa (30,850 ksi), a yield strength of 390 MPa (56,265 psi), and a tensile strength of 585 MPa (85,000 psi). It was assumed that the spike had a Poisson's ratio of 0.3, and density of 8050 kg/m^3 (0.029 lb/in.^{3}). Finally, the endurance limit was set at 233 MPa (33,800 psi) given it was assumed to be approximately 40% of the ultimate strength, which falls near the lower bound of the expected 35–60% range found within the literature [15]; thus leading to a conservative design.

The timber was modeled to account for the unique and independent mechanical properties in the directions of three mutually perpendicular axes: longitudinal (parallel to the direction of the timber fibers), tangential (perpendicular to the direction of the timber fibers and tangent to growth rings), and radial (perpendicular to the direction of the timber fibers and growth rings) [11]. To account

for this behavior, the validated timber user-defined material model (UMAT) developed by Sandhaas et al. [16,17] and previously deployed by Dersch et al. [4] was utilized. The modulus of elasticity was 11,376 MPa (1,650,000 psi), the compression and tension perpendicular to grain was 1.6 and 1.9 MPa (235 and 270 psi), respectively, and the compression and tension parallel to grain was 20.7 and 49.4 MPa (3000 and 7161 psi), respectively. Full model material details are presented by Dersch et al. [4].

The single rail seat model consists of either four or five cut spikes, a timber block, and a single plate. The plate modeled represents the current design standard for at least one North American heavy axle load (HAL) Class I railroad. The geometry was simplified in non-critical areas. Key fastening system components, their model representation, and mesh are presented in Fig. 5 and the details regarding element types and quantity of elements for each component are provided within Table 2.

The static coefficient of friction (CoF) between the cut spike and timber block as well as the plate and timber block was set at 0.7 [10]. The interactions between all components (e.g. spike and timber, plate and timber, etc.) were modeled as contact surfaces, and did not consider perfect bonding. And finally, boundary conditions were applied to all nodes of the bottom of all sleeper blocks restraining the displacement in the x, y, and z directions.

For additional details related to the validation which consisted of comparing laboratory recorded spike stress and displacement with respect to load data to model outputs of the single cut spike-timber block model, please refer to [4]. The authors believe the subsequent models (e.g. substitution of the screw spike or addition of additional spikes and plate) are iterations of this validated model.

4. Results and discussion

As mentioned previously, each model was used to quantify the effect of specific variables on the maximum spike stress when the fastener is subjected to a longitudinal load. For single spike studies (i.e. spike cross-sectional area, spike type, and effect of plate to spike contact location), each spike was subjected to a 11.12 kN (2500 lb.) longitudinal load. For the single rail seat studies (i.e. effect of normal clamping force and spike engagement with plate and quantity of spikes) each plate was subjected to a 11.12 kN (2500 lb.) longitudinal load; half the load was applied at one shoulder and the other half applied to the other (see arrows within Fig. 3 for approximate location of loads). These magnitudes were considered reasonable and selected because AREMA recommends that a fastening system withstand at least a 10.7 kN (2400 lb.) longitudinal load before rail slip for a single fastening system (or rail seat) [18] and the load is non-uniformly distributed within the spikes of fastening system [13].

4.1. Spike cross-Sectional area

Three spikes with square cross-sectional areas with widths of 15.88 mm (standard), 17.15 mm, and 18.42 mm (0.625 in. (standard), 0.675 in., and 0.725 in.) were investigated. Each was subjected to a 11.12 kN (2500 lb.) longitudinal load in increments and the maximum bending stress at each increment was recorded (Fig. 6). As expected, there was an inverse linear relationship between the increase in cross-section and maximum spike stress. Increasing the spike width from 15.88 mm to 18.42 mm (0.625″ to 0.725″) increases the cross-sectional area by 16%, increases the moment of inertia (I) by 81%, and resulted in the spike stress decreasing by 29%. Given the change in stress for the spike sizes investigated are linear, it can be seen that for each 1% increase in spike width from the standard spike there is approximately a 2% reduction in stress. Additionally, as the cross-section increases the longitudinal load magnitude required to exceed the endurance limit increases from approximately 8.67 kN (1950 lb.) to 11.12 kN (2500 lb.), or 22%. This trend is also linear and therefore for each 1% increase in spike width, there is approximately a 1.6% increase in the load required to exceed the endurance limit; thus, increasing resiliency and mitigating fatigue failures.

4.2. Spike type (cut vs screw)

Standard AREMA cut and screw spikes were both subjected to a 11.12 kN (2500 lb.) longitudinal load and the maximum stress was recorded. Fig. 7 provides a visualization of the stress distribution within each spike at a load of 11.12 kN (2500 lb.) applied. The data indicated that the maximum stress in the cut spike occurred at 39.4 mm (1.55 in.) while the maximum stress in the screw spike occurred at approximately 50.8 mm (2.00 in.) below the top of the crosstie. As presented by Dersch et al. [4] the depth of maximum stress for the cut spike increases as load increases. However, for the screw spike, the location of maximum stress was consistently at
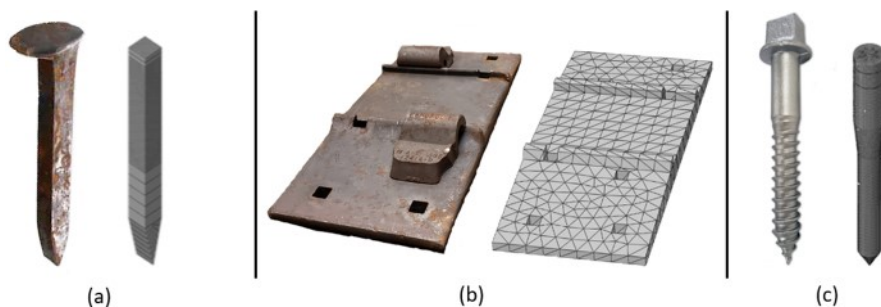

Fig. 5. Actual fastening system components and simplified model representation: (a) cut spike, (b) fastening system plate, and (c) screw spike.

Table 2
Model element type and meshing details.

Component		Element Type	Quantity of Elements			Hourglass Control
			Standard	0.675	0.725	
Spikes	Cut	C3D8R	9,936	10,816	12,544	–
	Screw	C3D8R	47,104	–	–	–
Plate	Standard	C3D10	2,218	–	–	–
Timber Blocks	Single Cut Spike	C3D8R	30,924	46,295	47,535	Yes
	Single Screw Spike	C3D8R	28,304	–	–	Yes
	Rail Seat	C3D8R	186,399	–	–	Yes
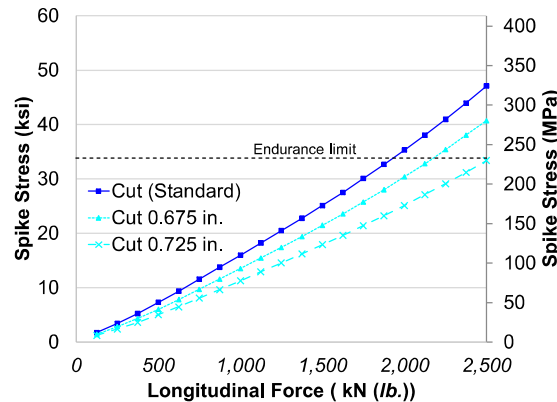
Fig. 6. Maximum bending stress of spikes with changing cross-sectional areas at various load magnitudes.

approximately 50.8 mm (2.00 in.) below the crosstie surface for the screw spike, or right at the bottom of the transition from the upper shank to the threads. This aligns with the results from modelling by Dick et al. [5] as well as field investigations findings screw spikes break at the first thread approximately 50.8 mm (2.00 in.) below the top of sleeper.

The maximum stress from each loading increment (Fig. 8) indicate that at longitudinal loads below 8.90 kN (2000 lb.) there is less than 10% difference in the maximum stress between the two spike types. However, beyond 8.90 kN (2000 lb.) the stress in the screw spike increases at an accelerating rate. This is likely driven by the stress concentration due to the abrupt change in geometry; thus, leading to plastic deformation of the spike. Further, given the lack of deviation below 8.90 kN (2000 lb.) there both spikes require the same magnitude of force to exceed the endurance limit. Therefore, for most expected loading scenarios, there is minimal difference in stress state or required load to exceed the endurance limit when comparing AREMA cut and screw spikes. However, for loads exceeding 8.90 kN (2000 lb.) the stress in the cut spike can be as much as 25% lower and the fatigue life of the screw spike would be lower. Additional work could investigate the effect of the simultaneous application of lateral and longitudinal loads to compare to these
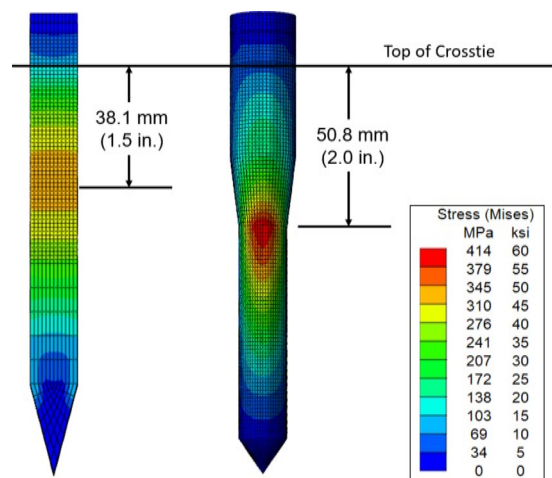

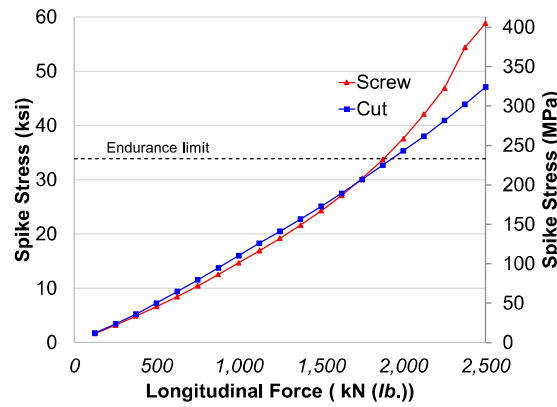**Fig. 7.** Qualitative surface stress comparison between cut and screw spike at 11.12 kN (2500 lb.)

Fig. 8. Maximum bending stress of cut and screw spike at various loading levels.

results.

4.3. Effect of plate to spike contact location

The AREMA cut spike was again subjected to longitudinal loads up to a maximum of 11.12 kN (2500 lb.). For the standard load case, the centroid of loading was 6.35 mm (0.25″) above the top of crosstie (the standard case assuming a uniformly distributed load over a 12.7 mm (0.5 in.) deep plate hole). However, to account for changes in load location this centroid location was changed to 12.1 mm (0.475 in.) above the top of the crosstie (i.e. High Contact) and 0.635 mm (0.025 in.) above the top of the crosstie (i.e. Low Contact). The load was applied over a surface in each instance. The surface area of the standard case was 202 mm^2 (0.3125 in.^{2}) (15.9 mm × 12.7 mm, (0.625 in. × 0.5 in.)). The surface area of both the high and low contact cases was 20.2 mm^2 (0.3125 in.^{2}) (15.9 mm × 1.27 mm, (0.625 in. × 0.05 in.)).

The maximum bending stress was recorded at each load increment (Fig. 9) for each case. The data indicate that there is a direct linear relationship between the change in load location and maximum stress. Quantitatively, regardless of applied load magnitude, there is approximately a ±20% change from the control case when the load location moves up and down, respectively. Additionally, when comparing the load required to exceed the endurance limit, there is also approximately a 20% increase or decrease when changing from the standard contact position to the high or low contact positions, respectively.

4.4. Effect of normal clamping force

The single fastening system model was subjected to a maximum longitudinal load of 11.12 kN (2500 lb.) while the magnitude of normal clamping force was increased from 4.45 kN/spike to 15 kN/spike (1000 lb./spike to 3370 lb./spike). The 15 kN/spike (3370 lb./spike) represents a case after initial installation and minimal settling. The 4.45 kN/spike (1000 lb./spike) represents a case where there would be a uniform 1 mm (0.039 in.) cutting of the plate into the sleeper or uniform loosening of the spikes.

Given previous results and literature indicate that the stress in the spike can vary for a variety of factors (e.g. loading location, spike
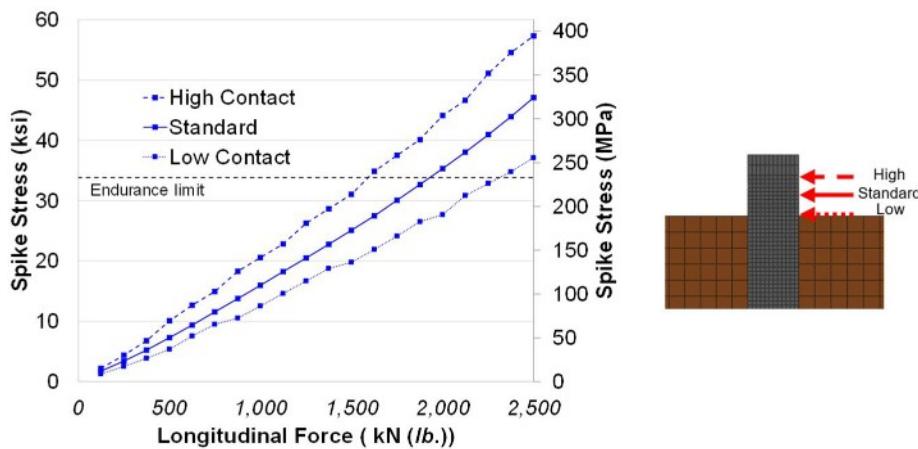

Fig. 9. Maximum bending stress of spikes at various loading levels and load locations.

orientation, load magnitude, etc.), a normalized stress value is reported for each case. A stress of "1" is the average stress distributed over four engaged spikes with the standard spiking pattern and no normal clamping force applied. The maximum spike stress data was recorded when the maximum longitudinal load was applied (Fig. 10).

When the clamping force per spike was 15 kN (3370 lb.) there is an 80% reduction in spike stress, on average. Further, even when there is additional settlement of the plate or loosening of the spikes, and the clamping force per spike was 4.45 kN (1000 lb.) (i.e. a 70% reduction in normal clamping force from the 15kN case), there is still a 70% reduction in spike stress (on average) from the control case. This 70–80% reduction indicates most longitudinal force would be taken by friction when introducing methods to apply a vertical normal force between the plate and sleeper. Developing friction at this interface aligns with design fundamentals for bolted shear joints that are expected to transfer load through a combination of friction and bearing [19].

4.5. Spike engagement with plate and quantity of spikes

The single fastening system model was subjected to a maximum longitudinal load of 11.12 kN (2500 lb.) as presented above. A normalized stress value is reported for each case where a stress of "1" is the average stress distributed over four engaged spikes installed with the standard spiking pattern. The maximum spike stress in each condition was then compared to this average baseline stress. The maximum spike stress data was recorded when the maximum longitudinal load was applied and a single spike was disengaged from the load path (Fig. 11).

In all cases studied, there is non-uniform force distribution within the fastening system. This can likely be attributed to the asymmetric placement of spikes relative to the point of loading. Further, it is evident that even though the fourth spike is present in each case, given the tolerances of the hole in the plate (e.g. 17.53 mm or 19.05 mm (0.69 in. or 0.75 in.)) are greater than the expected deflection of any spike (1.02 mm at 8.90 kN (0.04″ at 2,000 lb.)), the spike behaves as if it has been removed. The force the removed spike was carrying is not evenly distributed among the remaining spikes. Rather, the load is carried primarily by the adjacent spike. Regarding magnitude, when a single spike is removed from the load path, the adjacent spike's stress can increase by up to approximately 140% (or 2.4 times). It is believed that this more than doubling is driven by the plate rotation which changes the contact point between the spike and plate and thus introduces additional stresses into the spike.

The quantity of engaged spikes was changed (i.e. 3, 4, and 5) and the maximum spike bending stress was recorded when the maximum longitudinal load was applied (Fig. 12).

The addition of the fifth spike reduced the stress within spikes 3 and 4 but not of spikes 1 or 2. Therefore, even in the unlikely scenario of all spikes being engaged, increasing the number of spikes will not ensure a uniform reduction in maximum stress. Therefore, if spike engagement cannot be ensured, other methods to transfer the forces should be developed as discussed above (e.g. friction between the plate and sleeper).

5. Conclusions

To mitigate spike fatigue failures through the reduction in spike stresses, this paper presents the results from multiple, novel finite element analysis studies representing various fastening system conditions that affect the spike stress magnitude. The two most effective methods for reducing spike stress, thus mitigating spike failures, is to ensure spike engagement between the plate and spikes and the development of friction between the plate and sleeper (e.g. spring washers, etc.). Results also indicate that changes in spike type, cross-sectional area, quantity of spikes, and loading location have an effect, though not as significant as the engagement of spikes and development of plate to sleeper friction. Following is a summary of the novel findings stemming from this investigation:

- There is an inverse relationship between plate-sleeper normal clamping force and spikes stress
  o For example, a clamping force of 4.5 kN (1,000 lbs.) at each spike can lead to a 70% reduction in spike stress
- The disengagement of a single spike (reduction from 4 to 3) can lead to a 140% (2.4 times) increase in the stress experienced by a remaining spike
- There is little difference in cut and screw spike expected performance (load required to exceed fatigue limit) or strength (capacity) at longitudinal loads below 8.90 kN (2000 lb.)
- There is an inverse linear relationship between spike cross-section and resulting stress as well as load required to exceed the endurance limit
  o For each 1% increase in spike width from the standard spike condition there is approximately a 2% reduction in stress
  o For each 1% increase in spike width, from the standard spike condition there is approximately a 1.6% increase in the load required to exceed the endurance limit
- There is an inverse linear relationship between spike contact location and resulting stress as well as load to exceed the endurance limit
  o A ±6.22 mm (0.245″) change in load location can lead to approximately a −/+ 20% change in maximum stress and load required to exceed the endurance limit

These findings align with recommendations originally proposed by AREA and furthered by Kerr [9], fastening systems installed in demanding locations should employ fasteners whose only function is holding down the tie-plate to the tie and not transferring additional loads from the rail. Future fastening system designs can consider these results to mitigate spike fastener failures. That is, fasteners should be designed to transfer forces via friction when possible, encourage uniform engagement of the spikes, as well as
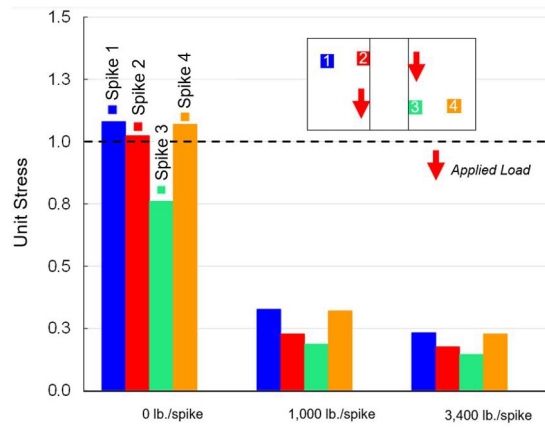
Fig. 10. Effect of normal clamping force on maximum spike stress at 11.12 kN (2500 lb.) longitudinal load application.
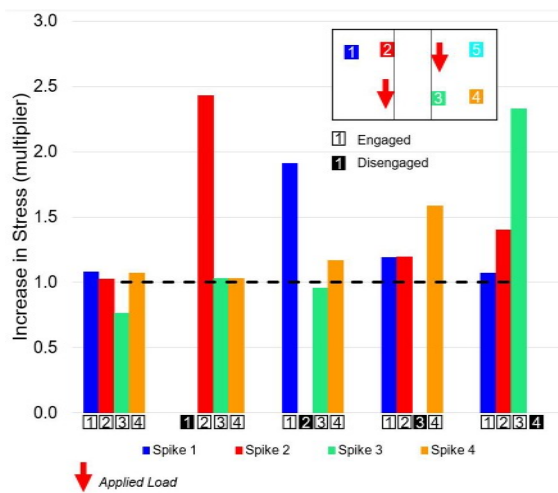

Fig. 11. The effect of spike engagement on maximum spike stress at 11.12 kN (2500 lb.) longitudinal load application with disengagement of one spike at a time.
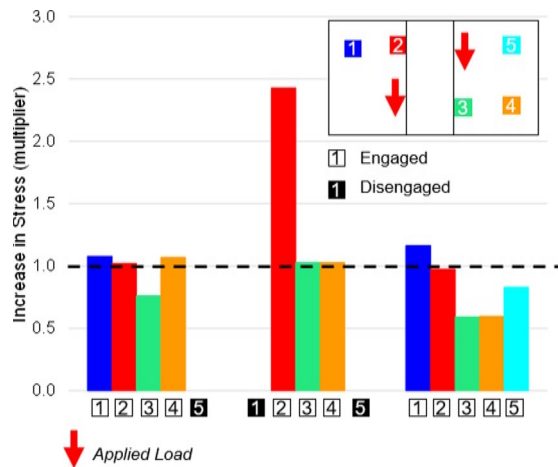

Fig. 12. The effect of quantity of spikes engaged on maximum spike stress under a longitudinal load application of 11.12 kN (2500 lb.)

encouraging forces to be transferred as close to the sleeper top surface as feasible. If additional capacity is still required, increasing the spike size could be considered.

Declaration of Competing Interest

The authors declare that they have no known competing financial interests or personal relationships that could have appeared to influence the work reported in this paper.

References

[1] W.W. Hay, Railroad engineering [Internet]. 2nd ed. Vol. 1. New York, NY, USA: John Wiley & Sons, 1982 [cited 2017 Mar 10]. Available from: https://books.google.com/books?hl=en&lr=&id=ygKio-Ks0doC&oi=fnd&pg=PA1&dq=hay+railroad+engineering&ots=AIb7mDxewk&sig=NfsAJ6fVwnLl3eKMGsT7R42Rm6Q.

[2] J.H. Armstrong, Chapter 3 – The track: alignment and structure, in: The Railroad: What It Is, What It Does. 5th ed. Omaha, NE, USA: Simmons Boardman, 2008, p. 21–50.

[3] C. Stuart, T.A. Roadcap, M. Dersch, Timber Crosstie Spike Fastener Failure Investigation. Federal Railroad Administration, Office of Research and Development; 2019 May p. 4. Report No.: 19–14.

[4] M. Dersch, T. Roadcap, J.R. Edwards, Y. Qian, J.-Y. Kim, M. Trizotto, Investigation into the effect of lateral and longitudinal loads on railroad spike stress magnitude and location using finite element analysis, Eng. Fail. Anal. 104 (2019) 388–398.

[5] M.G. Dick, D.S. McConnell, H.C. Iwand, Experimental measurement and finite element analysis of screw spike fatigue loads, in: Proceedings of the 2007 Joint Rail Conference and Internal Combustion Engine Division Spring Technical Conference [Internet]. Pueblo, CO, USA: American Society of Mechanical Engineers (ASME), 2007 [cited 2018 Jun 12]. p. 161–6. Available from: http://proceedings.asmedigitalcollection.asme.org/proceeding.aspx?articleid=1591004.

[6] Y. Gao, M. McHenry, B. Kerchof, Investigation of broken cut spikes on elastic fastener tie plates using an integrated simulation method. Proceedings of the 2018 Joint Rail Conference, 2018.

[7] T. Roadcap, B. Kerchof, M.S. Dersch, M. Trizotto, J.R. Edwards, Field experience and academic inquiry to understand mechanisms of spike and screw failures in railroad fastening systems. Proceedings of the 2019 AREMA Annual Conference with Railway Interchange, AREMA, Minneapolis, MN, 2019.

[8] M.S. Dersch, M. Trizotto Silva, J.R. Edwards, A. de O Lima, T. Roadcap, Analytical method to estimate railroad spike fastener stress, Res. Rec. J. Transp. Res. Board. 2674(11) (2020) 11.

[9] A.D. Kerr III, The evolution of track components, in: Fundamentals of Railway Track Engineering. Simmons Boardman, Omaha, NE, USA, 2003, p. 25–84.

[10] Forest Products Laboratory, Wood Handbook, Wood as an Engineering Material. Centennial Edition. United States Department of Agriculture, Forest Service, Madison, WI, 20509 p.

[11] G. Gurfinkel, Wood Engineering. Second. Kendall/Hunt Publishing Company, Dubuque, IA, USA, 1981, 558 p.

[12] R. Bowman, Internal NS Report, Reduce Spike Breakage, 2002.

[13] Y. Gao, J. LoPresti, Interim Report Broken Spike Remediation, Transportation Technology Center, Inc., Pueblo, CO, USA, 2020 Apr p. 4. Report No.: TD-20-004.

[14] American Railway Engineering and Maintenance-of-Way Association (AREMA). Chapter 5, Track. In: Manual for Railway Engineering. The American Railway Engineering and Maintenance-of-Way Association, Landover, MD, USA, 2017.

[15] F.C. Campbell, Chapter 14. Fatigue, in: Elements of Metallurgy and Engineering Alloys. ASM International, Materials Park, OH, USA, 2008.

[16] C. Sandhaas, 3D Material Model for Wood, Based on Continuum Damage Mechanics User Subroutine UMAT, TU Delft, Stevin laboratory, Delft, Netherlands, 2011 Nov. Report No.: 6-11–4.

[17] C. Sandhaas, Mechanical Behaviour of Timber Joints with Slotted-in Steel Plates [Doctoral Thesis], Delft University of Technology, Delft, Netherlands, 2012.

[18] American Railway Engineering and Maintenance-of-Way Association (AREMA). Chapter 30, Ties, in: Manual for Railway Engineering, The American Railway Engineering and Maintenance of Way Association, Landover, MD, USA, 2015.

[19] J.H. Bickford, Introduction to the Design and Behavior of Bolted Joints: Non-Gasketed Joints [Internet]. Fourth, CRC Press, Boca Raton, FL, USA, 2007 [cited 2020 May 1]. Available from: https://www.taylorfrancis.com/books/9780849381874.